Eur. Phys. J. B **44**, 447–454 (2005)
DOI: 10.1140/epjb/e2005-00144-1

THE EUROPEAN PHYSICAL JOURNAL B

EPR study of Mn^{2+} doped nanocrystalline PbF_2

P. Thangadurai[1], S. Ramasamy[1,a], T.K. Kundu[2], and P.T. Manoharan[2,b]

[1] Department of Nuclear Physics, University of Madras, Guindy Campus, Chennai 600 025, India
[2] Regional Sophisticated Instrumentation Centre, Indian Institute of Technology Madras, Chennai 600 036, India

Received 19 November 2004
Published online 30 May 2005 –

Abstract. Nanocrystalline samples of PbF_2 doped with 0.05, 0.1, 0.4 and 1 mol% Mn^{2+}, used as paramagnetic probe, were prepared by inert gas condensation technique. All the samples were vacuum annealed at different temperatures to get different grain sizes. The X-ray diffraction studies showed the dominant content of β-PbF_2 phase with a fractional quantity of α-PbF_2. Thermal stability and sublattice melting were studied by TGA and DSC respectively. EPR measurements were made on all these samples at 77 and 300 K. The EPR spectra of all samples were found to contain well resolved sextet arising from the Mn^{2+} ions that occupied the cubic sites of Pb^{2+} ion of PbF_2 lattice. The lower concentration of the Mn^{2+} ions (0.05 and 0.1 mol%) clearly monitored the Pb^{2+} environment in the PbF_2 lattice. The 0.4 mol% showed the presence of only the cubic sites with a minor concentration of the orthorhombic sites. The spectra corresponding to 1 mol% Mn^{2+} clearly showed two different components. The isotropic nature of the 1 mol% as-prepared sample implied that there was no cluster formation and hence this EPR spectrum was taken as the single ion spectrum. The annealed samples contain two spectral components; one is from the isolated single ions and the other one from the Mn^{2+} clusters. The spectral component of Mn^{2+} clusters was obtained by subtracting the spectrum for the as-prepared sample for the spectra of annealed samples. The extracted cluster phase spectra and the pure spectrum from the as-prepared sample were then combined to simulate the entire set of experimental spectra. The simulated spectra were found to be in good agreement with the experimental data. The g values obtained were in the range very close to the free electron g factor as the electrons are in the S state ($L = 0$).

PACS. 81.07.Wx Nanopowders – 61.46.+w Nanoscale materials: clusters, nanoparticles, nanotubes, and nanocrystals – 61.10.Nz X-ray diffraction – 81.70.Pg Thermal analysis, differential thermal analysis (DTA), differential thermogravimetric analysis – 76.30.-v Electron paramagnetic resonance and relaxation

Introduction

Due to the advantageous changes in physical and chemical properties of nanocrystalline materials [1], they are of prime interest to the researchers as well as to the technologists. Lead (II) fluoride (PbF_2) is a well-known superionic conductor and it is used as a solid-state electrolyte [2,3] in solid-state batteries. Not much of work at the nano level of PbF_2, specifically on the application to these properties, have been researched and hence our interest in this subject. It exists in two polymorphs, one is the high-pressure orthorhombic α-PbF_2 and the other is the cubic (fluorite structured) β-PbF_2. The structural phase conversion from α to β can be achieved by heating the samples at high temperature around 610 K for one hour [4] and the reverse is achieved by applying a high pressure of the order of 4 kbar [5]. Many works on this material using nuclear magnetic resonance have been carried out on both ^{207}Pb [6,7] and ^{19}F [8] nuclei of PbF_2 as both of them are NMR active.

Electron paramagnetic resonance (EPR) technique is a good tool to study certain atomic and molecular systems having a paramagnetic moment. EPR studies on doped fluorides have been reported earlier to study the defect structures and the defect-defect interactions [9,10]. Lead fluoride by itself is an EPR inactive as both ions are non-magnetic, having closed shell electronic configuration. In the literature, one can find the practice of substituting paramagnetic ions like Mn^{2+}, Gd^{3+} etc. in the sites of Pb^{2+} (this method is called as 'magnetic tagging' [11] or 'magnetic doping') to study the environment of Pb^{2+} by EPR. Rose and Schneider [12] have studied the point defects on fluorine sites induced by gamma ray irradiation in cubic PbF_2 single crystals using EPR. ten Eicken et al. [13] have heterovalently doped Gd^{3+} ions in the lattice of β-PbF_2 both in single crystal and powder forms and studied their EPR spectra to correlate the spectral lines to different Gd sites and compared with

[a] e-mail: sinna_ramasamy@yahoo.com
[b] Honorary Professor, JNCASR, Bangalore, India

other Gd doped fluorite structured solid solutions [14]. In a V^{2+} doped PbF_2 a broad line EPR spectrum was obtained and that was associated to the impurity centers [15]. Chan and Shields [16] have studied the EPR of single crystal lead fluoride using Cr^{3+}, Mn^{2+}, Fe^{2+} and Fe^{3+} as paramagnetic probe. In this work, we have investigated the Mn^{2+} doped nanocrystalline $PbF_2$with the help of XRD, thermal analysis and EPR. In this work, Mn^{2+} was chosen as the paramagnetic probe of PbF_2 because of the following reasons as discussed by Evora and Jacarrino [17], who have studied Mn^{2+} doped PbF_2 single crystal using EPR: (1) Mn^{2+} may be introduced substitutionally for Pb^{2+}, (2) it couples weakly to the lattice, making relaxation broadening of the EPR in a harmonic solid insignificant at all temperatures, and (3) it has a large ^{55}Mn hyperfine splitting parameters A(^{55}Mn) as well as a transferred (superhyperfine) splittings A(^{19}F) between each Mn^{2+} ion and its eight nearest-neighbor (nn) F^{19} nuclei. The divalent manganese has five $3d$ electrons and a half filled electron shell. Therefore the resultant orbital angular momentum is $L = 0$ and spin angular momentum, $S = 5/2$. The paramagnetism arises only from these unpaired electronic spins. It is also attempted to separate the EPR lines originated from two different occupational positions of Mn^{2+} in the 1 mol% doped PbF_2.

Experimental details

Nanocrystalline PbF_2 doped with Mn^{2+} paramagnetic ions has been prepared by the inert gas condensation technique under ultra high vacuum (of the order of 10^{-8} Torr) conditions using the in-house developed ultra high vacuum chamber. The source materials PbF_2 (Sigma Chemicals Company, Inc. USA, with the purity 99.99%) and MnF_2 (Cerac Inc. USA, with the purity 99.9%) were taken to have 0.05, 0.1, 0.4 and 1.0 mol% of Mn^{2+}. The mixture was mechanically ground for an hour to get good homogeneity and then loaded in a molybdenum boat. It was evaporated by joule heating and the evaporated molecules were collected on the surface of a cold finger (a stainless steel cylindrical vessel) kept at 77 K. The helium gas with a pressure of 0.5 mbar was used as a carrier gas. The detailed method of preparation is similar to the one discussed elsewhere [6]. The as-synthesized nanopowders were annealed at four different temperatures (473, 573, 623 and 673 K) under a vacuum of the order of 10^{-5} Torr to get different grain sizes. X-ray diffraction (XRD) patterns were recorded using a Siefert powder X-ray diffractometer with Cu-$K_{\alpha 1}$ radiation. Grain sizes were calculated using the Scherrer formula [18].

Thermal properties of nanocrystalline Mn^{2+} doped PbF_2 have been studied by Differential Scanning Calorimetry (DSC) and Thermogravimetric analysis (TGA). DSC measurements were performed in the DSC 204 Phoenix of Netzsch Company in the temperature range from 300 to 773 K. The DSC calorimeter was calibrated against the melting point of indium. The TGA thermograms were taken using the thermal analyzer model STA 409 C of Netzsch in the temperature ranging from 300 to 1273 K. All the thermal measurements were made with the heating rate of 10 K/minute under dry nitrogen atmosphere.

EPR measurements were carried out at room temperature (300 K) and at 77 K, using the Varian E-112 EPR spectrometer in the scan range from 2400 to 4300 G. The microwave power used was 10 mW. The modulation amplitude and modulation frequencies were 5 G and 100 kHz respectively. The spectrum due to Mn^{2+} clusters in 1 mol% doped PbF_2 alone was extracted by subtracting out the EPR spectrum of the as-synthesized sample from the mixed component spectra of annealed samples in an appropriate manner. Thus obtained EPR spectrum of the cluster component is then superposed on the isolated Mn^{2+} component spectrum in different proportions to simulate the experimental mixed component spectra corresponding to annealing temperatures 473, 573, 623 and 673 K. The same procedure was adapted for both measurements at 300 K and 77 K of 1 mol% doped samples.

Results and discussion

X-ray diffraction study

Figures 1a to d give the X-ray diffraction patterns of respectively 0.05, 0.1, 0.4 and 1 mol% Mn^{2+} doped PbF_2. The annealing temperature and the grain size of each sample are given against the corresponding pattern. It is found from Figure 1 that the as-prepared samples contain purely cubic PbF_2 phase while the annealed ones contain a fraction of orthorhombic phase also. The relative concentration of the latter phase varies with annealing temperature. Though only one peak corresponding to the α phase is visible clearly in Figure 1, we can see few other peaks on zooming in. One such magnified XRD plot for 0.05 mol% doped and 673 K annealed sample is given as inset in Figure 1a for clarity. Figure 2 shows the variation of the grain size with the annealing temperature in all Mn^{2+} doped nanocrystalline PbF_2.

Thermal analysis

Figure 3 shows the TGA thermograms for 1 mol% Mn^{2+} doped nanocrystalline PbF_2. Up to 1173 K the sample shows good thermal stability. After 1173 K, above its melting point, the deep fall is observed and this fall may correspond to the beginning of evaporation of this material. Figures 4a and b show the DSC thermograms of the as-prepared PbF_2 with 0.05 and 0.1 mol% of Mn^{2+} content respectively measured in the temperature range from 323 to 773 K (DSC measurements for 0.4 and 1 mol% of Mn^{2+} were not done). There is one exothermic and one endothermic peak observed for both samples. The temperatures of the peaks are marked in the respective figures. Many works have been done on single crystal [19,20] and polycrystalline PbF_2 in both the phases [21] using

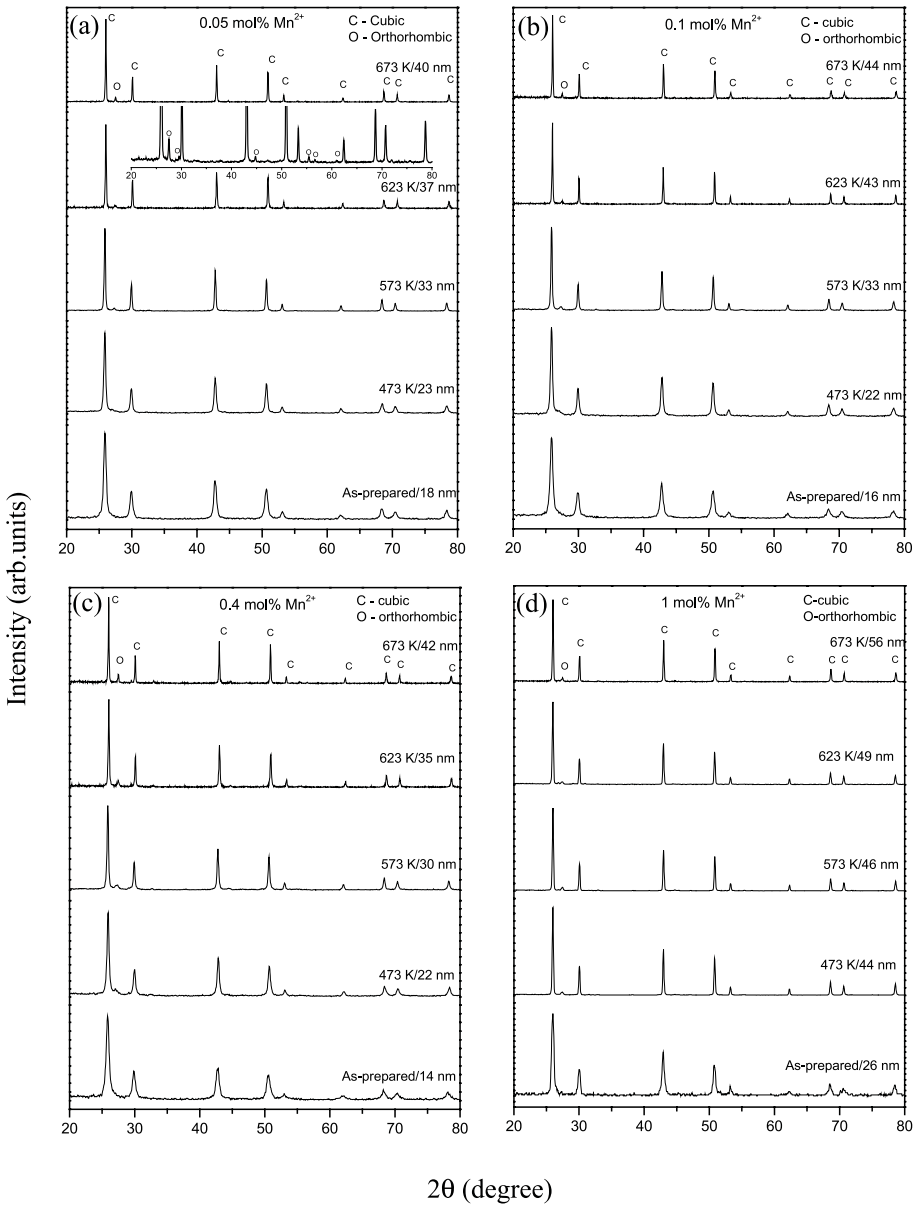

Fig. 1. X-ray diffraction patterns for the nanocrystalline PbF_2, with (a) 0.05, (b) 0.1, (c) 0.4 and (d) 1 mol% Mn^{2+} content, prepared by inert gas condensation technique. Annealing temperature and the grain size are given against each pattern. Inset in (a) is the magnified XRD pattern for 0.05 mol% and 673 K annealed sample.

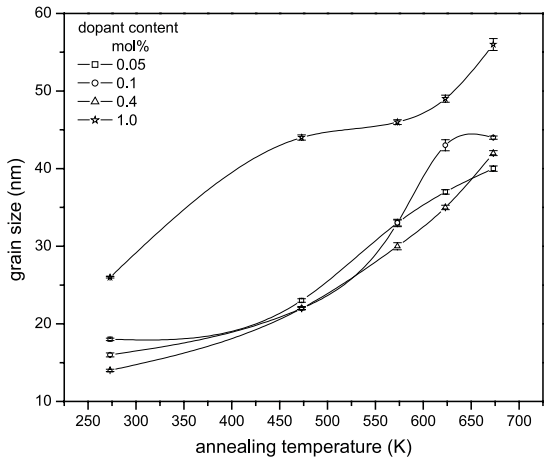

Fig. 2. Grain size versus annealing temperature for Mn^{2+} doped nanocrystalline PbF_2 as calculated from the X-ray diffraction pattern. Lines are guide to eyes.

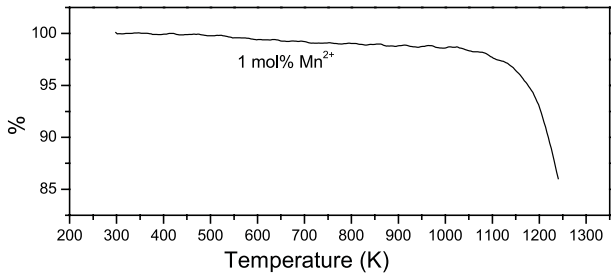

Fig. 3. TGA thermogram for 1 mol% Mn^{2+} doped nanocrystalline PbF_2.

DSC and DTA measurements. There have been many attempts to relate the enthalpy to the superionic transitions occurring in compounds having the fluorite structure [22,23]. These enthalpy determinations indicate that the transitions to the superionic state are quite evident and may be of second order. The first exothermic peak

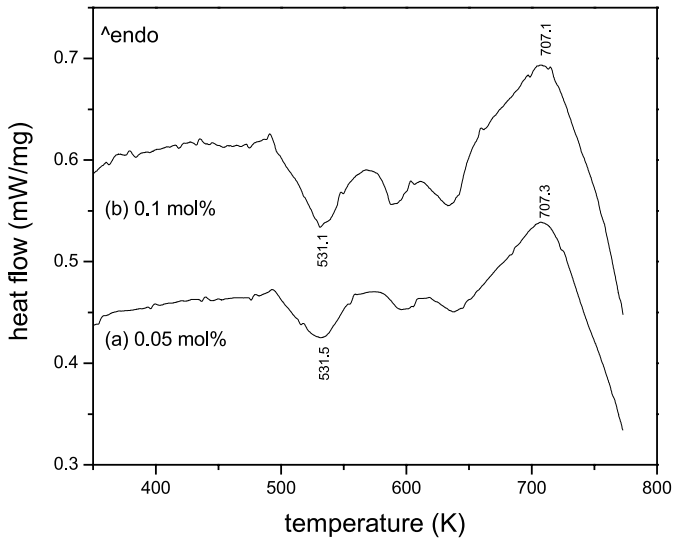

Fig. 4. DSC curves for (a) 0.05 mol% and (b) 0.1 mol% Mn^{2+} doped nanocrystalline PbF_2. Peak temperatures are noted in K.

in 0.05 and 0.1 mol% doped samples respectively at 531.5 and 531 K may be due to crystallization of some amorphous phases present in these samples. The endothermic peak was observed at 707.3 K and 707.1 K for 0.05 and 0.1 mol% doped PbF_2 samples respectively. This endothermic peak at 707 K can be attributed to the transition from normal conducting state to the superionic conducting state. This peak is very broad as the sublattice melting process is not a sharp transition in fluorite structures [21]. During sublattice melting F^- ions will leave from its lattice site forming Frenkel defects leading to high-conducting superionic state.

Electron paramagnetic resonance studies

Figures 5a, b, c and d show the room temperature EPR spectra of the nanocrystalline PbF_2 with 1, 0.4, 0.1, and 0.05 mol% of Mn^{2+} concentration respectively. Their corresponding spectra measured at 77 K are given in Figures 5e, f, g and h respectively. Each figure contains the spectra of the as-prepared and annealed samples with particular composition. All the spectra showed well-resolved sextet originating from the interaction between ^{55}Mn nucleus of spin $I = 5/2$ and its unpaired electrons. Though all the spectra showed sextet corresponding to the Mn^{2+} ion, the line shapes of the spectra assume different characteristics with respect to dopant concentration and grain sizes (annealing temperature). However, no superhyperfine lines could be observed possibly due to higher linewidth as well as longer Mn-F bond distance in these materials (2.55 to 2.77 Å) than what is normally observed in MnF_2 (2.11 to 2.14 Å) [24]. Already there are references on Mn^{2+} doped PbF_2 in which less than 10^{-4} mole of Mn^{2+} at a measuring temperature of 77 K alone produced a slightly resolved superhyperfine lines due to F^{19}. Even the 10^{-2} and 10^{-3} mole of Mn^{2+} could not give rise to the resolution of the superhyperfine lines [17].

We are able observe a definite concentration dependence of EPR spectra in our attempts to monitor the phase changes in the PbF_2 lattice doped with Mn^{2+}. For obvious reasons of concentration dependence and its consequence on the EPR properties and vice versa, we like to discuss the EPR spectral behaviour in order of decreasing dopant concentration since the lower doping by Mn^{2+} is proved to be a correct representation of phase changes as a function of annealing temperature in agreement with the other experimental evidences such as XRD.

From the EPR spectra (Figs. 5a–h), it is evident that there are two different types of EPR signals as a function of dopant concentration. At 0.4 mol% of Mn^{2+} concentration, the spectrum is mainly due to a single sextet ($I = 5/2$ of Mn^{2+} interacting with the unpaired electrons). But for 1.0, 0.1 and 0.05 mol% concentrations, there are at least two different environments. When Mn^{2+} is doped in PbF_2, in principle, there are two possible environments and, correspondingly, two types of Mn^{2+} EPR signals. One is that the paramagnetic species with divalent charge can replace substitutionally the cations and thereby sited in cubic symmetry surrounded by eight fluoride ions and produce no anisotropy. The second is the probability of the formation of Mn^{2+} clusters within its exchange distance. In addition to these two, in the case of tripositive ion substitution, charge compensation is required and hence the cubic symmetry may be reduced to trigonal, tetragonal or orthorhombic symmetry in which the crystal field axes may not necessarily coincide with the crystallographic axes.

Figures 5a and e give the EPR spectra of the 1 mol% Mn^{2+} doped nanocrystalline PbF_2 measured at RT and 77 K respectively. Here very interesting features are observed. As-prepared sample of this did not show any anisotropy as it contains only β-PbF_2 as observed from XRD and hence the impurity ions could substitute the cubic sites. But the annealed samples of 1 mol% dopant content showed two components. One may be from the isolated single Mn^{2+} ions and the other one may be originated from Mn^{2+} clusters formed due to higher dopant concentrations. The isolated single Mn^{2+} ions contain the resolved sextet. The broad resonance line may be from the Mn^{2+} clusters. This kind of spectra have been already reported for the Mn^{2+} substituted ZnS with the 1 mol% dopant [25,26]. Formation of Mn^{2+} clusters in PbF_2 can be justified in the annealed samples with 1 mol% dopant. During annealing, isolated Mn^{2+} can easily diffuse into another site and forming cluster. The possibility of the formation of Mn^{2+} clusters in ZnS with cubic structure has been thoroughly studied by Yeom et al. [25] and Lee et al. [26]. We argue in a similar way. The Mn^{2+} ions are substitutional impurities, which reside on normal Pb^{2+} ion lattice sites. It is therefore reasonable to expect any diffusion of Mn^{2+} in PbF_2 to occur by a vacancy diffusion mechanism. It looks that the clustering of Mn^{2+} ions contradicts the basic thermodynamic

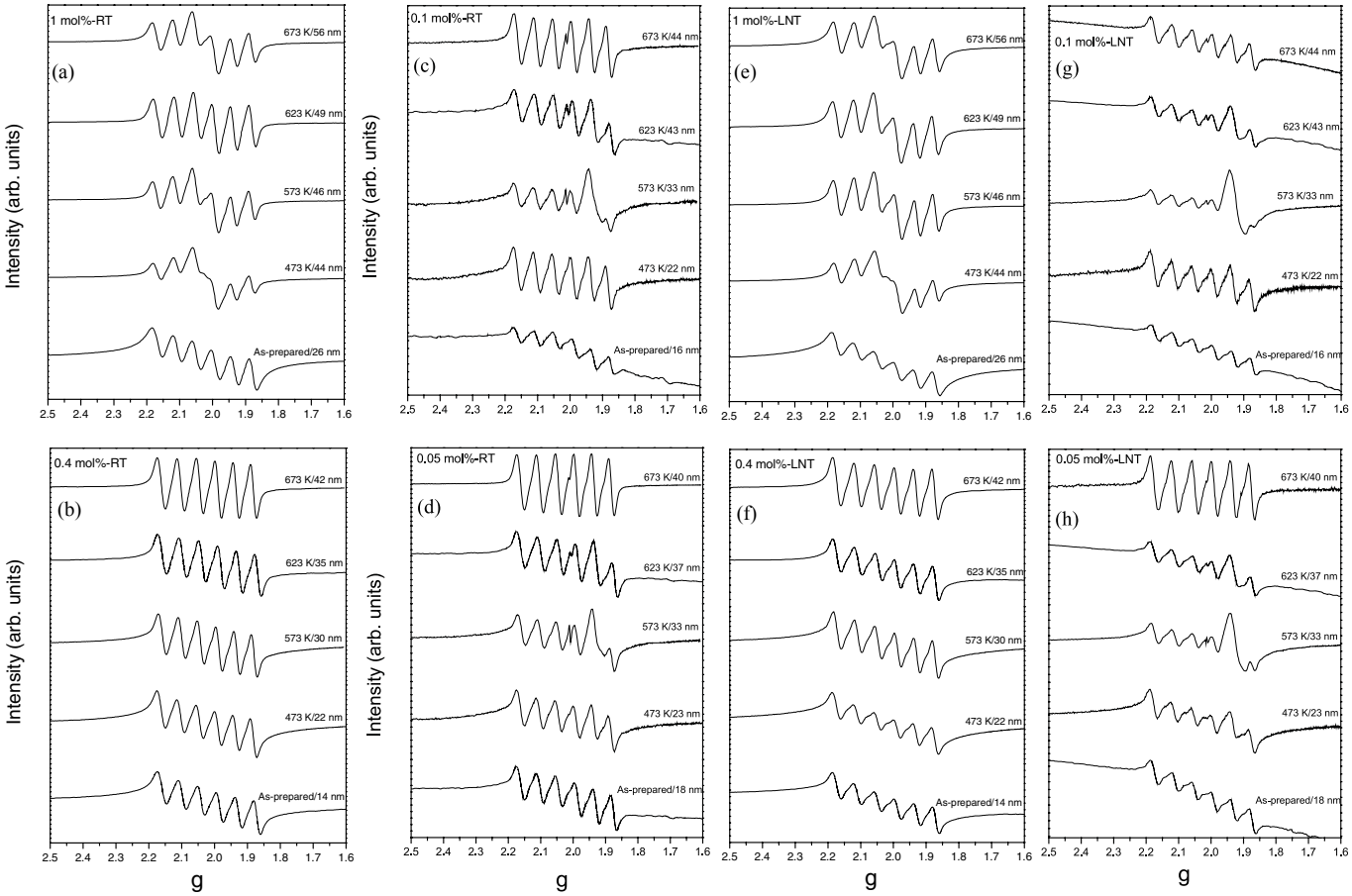

Fig. 5. Typical sets EPR spectra of the as-prepared and annealed nanocrystalline PbF_2 with Mn^{2+} concentration of (a) 1.0, (b) 0.4, (c) 0.1 and (d) 0.05 mol% measured at room temperature. The spectra (e), (f), (g) and (h) are their respective EPR spectra measured at 77 K. The six lines were originated from the ^6S state of Mn^{2+} probe ion. The annealing temperature and grain size are given against each spectrum.

requirement for a statistical uniform impurity distribution in the host lattice. However, from a quantum mechanical point of view, the substitution of Pb^{2+} (d^{10}) by an Mn^{2+} (d^5) impurity brings the electron deficiency. This electron deficiency can be resolved by delocalization of electron via bringing the Mn^{2+} ions closer in order to let them share the available electron [26,28]. If this is the case, then the orbital population and the symmetry restrictions should play a very important role in the clustering effect. The total energy lowering of the system due to clustering makes it favorable for Mn^{2+} ions to form clusters in the lattice and it is theoretically confirmed [26].

These two different environments lead to the different interactions of Mn^{2+} monitoring the site of Pb^{2+} giving different EPR lines. While the Mn^{2+} spectrum of the as-prepared samples is very clear and unique from Figures 5a and e respectively for 300 and 77 K, the spectrum due to the dopant clusters has been first carefully obtained by subtracting out the spectrum due to isolated ions from the 673 K spectrum due to two components. Thus the obtained Mn^{2+} cluster spectrum was then added to β phase in different percentages (or amounts) to simulate the experimental spectra of samples annealed at various temperatures. This is shown in Figures 6 and 7 respectively for the room temperature and 77 K experimental EPR data. In both figures, panel A gives the spectra of isolated ions (solid lines) and cluster (dashed line) and the panel B gives the experimental (solid line) and combined (dashed) spectra of these two components after addition in right proportion. In both cases it is clear that the spectra due to cluster are devoid of hyperfine lines due to exchange narrowing while the spectra due to the isolated ions has hyperfine lines due to ^{55}Mn ion. The agreement between experimental and generated spectra as shown in panel B of these figures is gratifying. For the samples measured at room temperature there was an exact match between the experimental and simulated spectra. For the samples measured at 77 K, other than the as-synthesized sample, a partial mismatch was observed between the generated and experimental spectra. The above discussion is true for both the EPR measurements done at 300 and 77 K

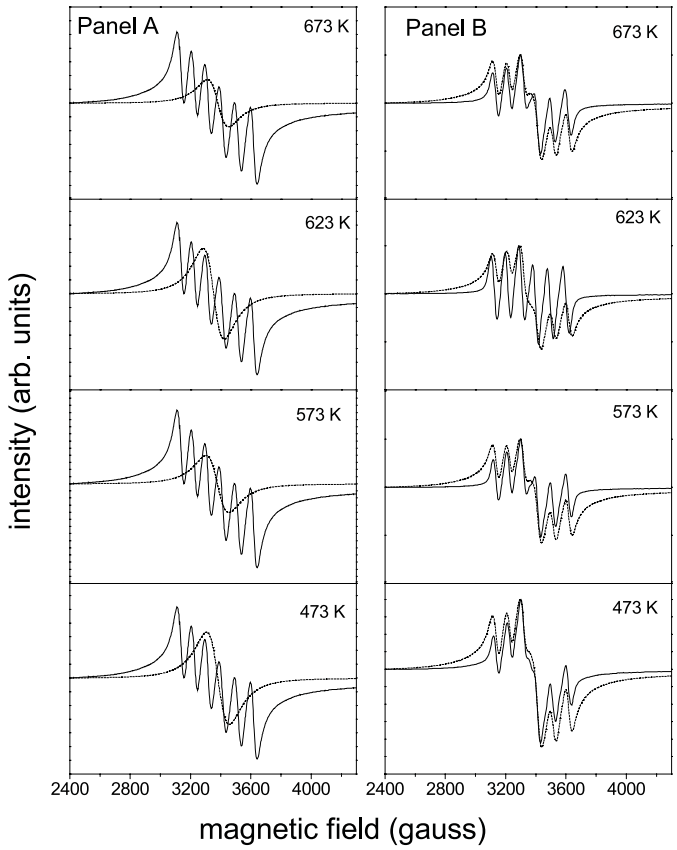

Fig. 6. Panel A: EPR spectral components of the isolated (6-line) and cluster Mn^{2+} ions (single line) for the 1 mol% Mn^{2+} doped nanocrystalline PbF_2 measured at room temperature. Panel B: The resultant spectra (dashed line) obtained by adding the two components in the amounts shown in Panel A are given along with their corresponding experimental EPR spectra (solid line). Annealing temperatures are given against each spectrum.

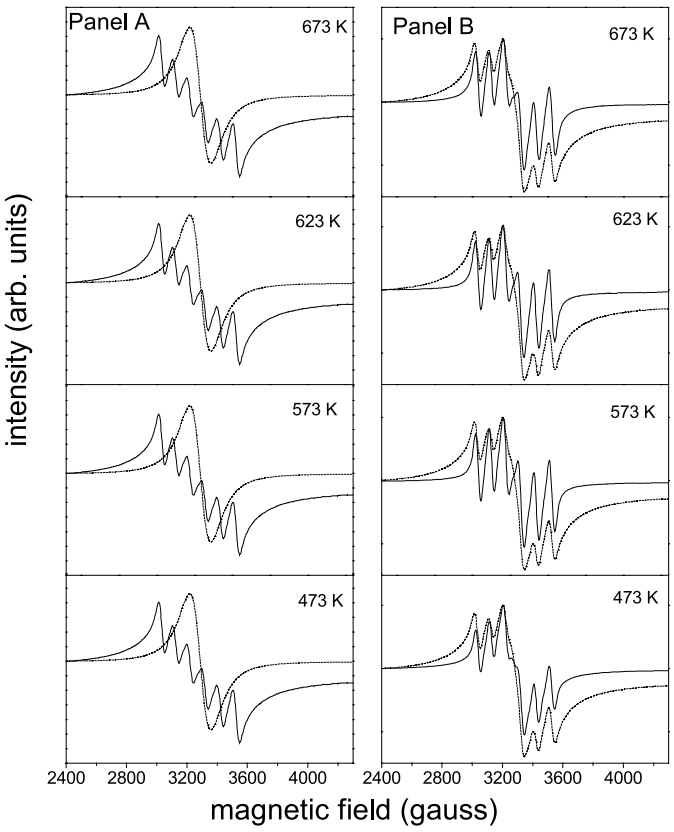

Fig. 7. Panel A: EPR spectral components of the isolated (6-line) and cluster Mn^{2+} ions (single line) for the 1 mol% Mn^{2+} doped nanocrystalline PbF_2measured at 77 K. Panel B: The resultant spectra (dashed line) obtained by adding the two components in the amounts shown in Panel A are given along with their corresponding experimental EPR spectra (solid line). Annealing temperatures are given against each spectrum.

of 1 mol% doped PbF_2, except for differing line widths. It is interesting to note that the linewidth of isolated ions spectrum is lower at 300 K than that at 77 K while the reverse is true for the cluster spectrum (ΔH = 120 G at 77 K and 130 G at 300 K). The decrease in linewidth at 77 K for the cluster may be due to a slight contraction of the Pb(Mn)-F bond distance and hence the lattice, thereby increasing the exchange narrowing. It is necessary to point out that this broadening is not due to microwave power saturations (vide supra, experimental procedure). An additional possibility is phonon decoupled exchange at lower temperatures.

A look at the EPR spectra at all annealing temperatures of 0.4 mol% doped PbF_2 in Figures 5b and f shows only a well resolved sextet. The central single exchange narrowed line due to cluster formation as in 1 mol% doped samples was not observed here. The sextet showed that the impurity ions have been substituted mostly in the cubic sites and may be also in the orthorhombic sites to a minor extent. Hence, all such Mn^{2+} ions found in clusters in Figure 5a have now gone in as isolated ions, increasing the relative concentration of the latter. Yet another observation was a substantial decrease in linewidth of the hyperfine spectra as the grain size increases with annealing temperature, revealing an increased crystallinity of the samples.

The 300 and 77 K measured EPR spectra in Figures 5c, d, g and h for 0.1 and 0.05 mol% doped PbF_2 showed the presence of isolated Mn^{2+} ions substituted in the cation sites. As-prepared and 473 K annealed samples in both cases showed the presence of only one set of isotropic hyperfine lines due to ^{55}Mn indicating that all the Mn^{2+} ions have been substituted in the cubic sites (β). But at higher annealing temperatures above 473 K, the EPR spectra started showing more than one set of EPR spectra. In addition to the sextet as observed at higher dopant concentration as well as at this reduced concentration both for as-prepared and for 473 K annealed case, we also observe (i) the emergence of a sharp isotropic line at $g = 2$ and a broad and intense line at $g \sim 1.95$; (ii) both these lines decrease in intensity with increased annealing

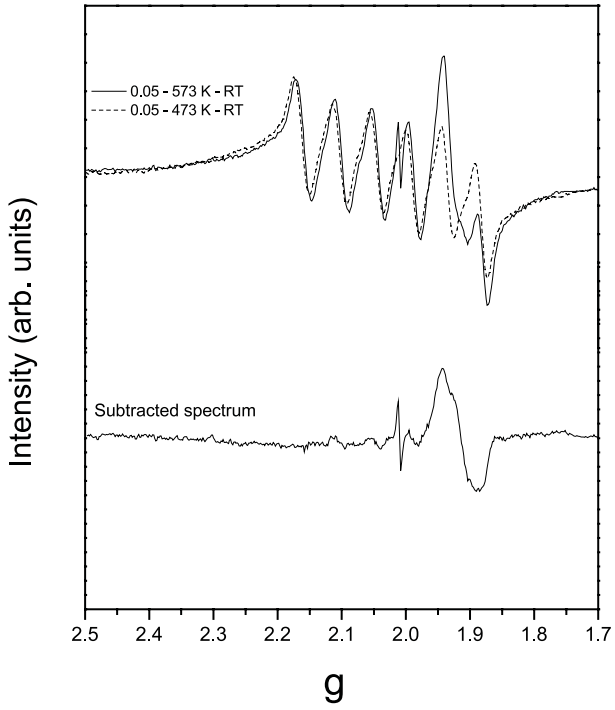

Fig. 8. Experimental EPR spectra for the 473 K (dashed line) and 573 K (top solid line) for the 0.05 mol% doped PbF_2. The subtracted spectrum (explained in the text) is given at bottom.

temperature; (iii) at the highest annealing temperature of 673 K, the disappearance of the new lines (though a very minor constituent of the sharp line ($g = 2$) still present) is synchronous with the sharpening of the sextet. To clearly demonstrate the differential nature of observation (i), we have subtracted the 473 K spectrum (sextet) from the 573 K spectrum; the results are shown in Figure 8. While the sextet is due to the doping of Mn^{2+} in the cubic β-phase, the sharp line at $g = 2$ is due to doping in α-phase, as proven by earlier observation of its decreasing concentration at higher annealing temperatures [5,26–28]. The lack of hyperfine lines and its sharpness as seen in Figure 8 for this constituent in the α-phase are due to long Mn-F bond and consequent weak interaction possibly leading to free rotation of Mn^{2+} ion. However, the broader line formation may be due to one of the following possibilities. (i) It is due to the presence of Mn^{2+} in grain boundary with possible dangling bonds, which means reduction in the symmetry of Mn^{2+} and hence Pb^{2+} environment leading to the observed lower g value. As the annealing temperature increases, the grain boundary decreases due to the improvement of crystallinity. The resulting Mn^{2+} substitutes Pb^{2+} going into β-phase affecting the ratio of β and α contents in favour of the former and hence a decrease in the intensity of the sharp line at $g = 2$. As a result, better crystalline condition at high annealing temperature distributes the Mn^{2+} in isolated cubic sites, leading to a reduction in the linewidth and hence the sharp 6-line EPR spectrum. (ii) The second possibility for the simultaneous appearance of the sharp line at $g \sim 2.01$ and the broad signal at $g \sim 1.95$ may be due to the former belonging to defects having dangling bonds and the latter due to Mn^{4+} ions in grain boundary. Usually the latter has g-value below 2.0 [29]. (iii) The third possibility for the appearance of a broad line especially at a lower g-value of $\sim$1.95 is due to its origin from a F centre, in the near presence of higher atomic number element Pb. This possibility has other corroborative evidences: (i) the g-value of F-centres in CaO, SrO, BaO decreases in the order 2.0, 1.984 and 1.938 [30]; (ii) the presence of electronic centres in pure PbF_2 has been proved to be present, by both Raman and Photoluminescence spectroscopy [31]; (iii) as expected, the electronic centres formed on heating at 473−573 K disappear totally at 673 K, a case of bleaching at high temperature. In this case, the sharper line must have been due to the presence of Mn^{2+} ions with F^- ions at longer distances as in the case (i) discussed above. Of the three possibilities, the third seems to be the most probable.

The values of spectroscopic splitting factor g and hyperfine structure constant A as obtained from the experimental spectra are in the normally expected range of $g \sim 2.0 \pm 0.001$ and $A \sim 92 \pm 1$ G. This is due to the fact that the Mn^{2+} ions do not have orbital angular momentum and the electrons are in the S state as they have a half filled d level.

Conclusion

Nanocrystalline PbF_2 doped with four different Mn^{2+} concentrations were prepared by inert gas condensation technique and annealed under vacuum to get different grain sizes. The XRD patterns showed α and β phases of PbF_2. The TGA and DSC showed the thermal stability and the superionic phase transition respectively. EPR spectra with different nature were observed as a function of dopant content and grain size. Isolated Mn^{2+} ions got substituted when the dopant content was low and formed Mn^{2+} clusters at highest dopant content studied. The 1 mol% doped PbF_2 contained two components corresponding to the isolated and correlated clustered Mn^{2+} ions. The sextet and the separated single line spectra have been attributed to the single ion and the clustered Mn^{2+} ions respectively. At the same time, it is evident that low dopant concentrations for EPR studies can alone reveal the real phase transitional feature and grain boundary behaviour of PbF_2 lattice. The experimentally observed and the generated spectra for the mixed components showed good agreement.

The support extended by the DST (Scheme, SR/S5/NM-58/2002) and COSIST programmes are gratefully acknowledged. One of the authors (PT) acknowledges the financial support from CSIR-India by the award of SRF (9/115(565)/2002-EMR-I). The author PTM thanks the DST, India for a scheme (SP/S-1/F-18/2000).

References

1. H. Gleiter, Prog. Mater. Sci. **33**, 223 (1989)
2. J.H. Kennedy, R. Miles, J. Hunter, J. Electrochem. Soc.: Electrochem. Sci. Tech. **120**, 1441 (1973)
3. N. Egashira, H. Kokado, Jpn J. Appl. Phys. **25**, L462 (1986)
4. G.A. Samara, Ferroelectrics **17**, 357 (1977)
5. G.A. Samara, J. Phys. Chem. Solids **40**, 509 (1978)
6. P. Thangadurai, S. Ramasamy, P.T. Manoharan, Eur. Phys. J. B **37**, 425 (2004)
7. F. Fayon, I. Farnan, C. Bessada, J. Coutures, D. Massiot, J.P. Coutures, J. Am. Chem. Soc. **119**, 6837 (1997)
8. F. Wang, C.P. Grey, J. Am. Chem. Soc. **120**, 970 (1998)
9. H.W. Den Hartog, Phys. Rev. B **27**, 20 (1983)
10. W. Low, Phys. Rev. **105**, 793 (1957)
11. R. Hogg, S.P. Vernon, V. Jaccarino, Phy. Rev. Lett. **39**, 481 (1977)
12. B. Rose, E. Schneider, Phys. Lett. A **34**, 27 (1971)
13. J. ten Eicken, W. Gunsser, S.V. Chernov, I.V. Murin, Ber. Bunsenges. Phys. Chem. **96**, 1723 (1992)
14. J. ten Eicken, W. Gunsser, S.V. Chernov, A.V. Glumov, I.V. Murin, Solid State Ionics **53-56**, 843 (1992)
15. K.K. Chan, L. Shields, J. Phys. C: Solid State Phys. **3**, 292 (1970)
16. K.K. Chan, L. Shields, J. Phys. C: Solid State Phys. **2**, 1978 (1969)
17. C. Evora, V. Jaccarino, Phy. Rev. Lett. **39**, 1554 (1977)
18. B.D. Cullity, in *Elements of X-ray Diffraction* (Addison-Wesley, 1977), p. 81
19. J.P. Goff, W. Hayes, S. Hull, M.T. Hutchings, J. Phys.: Condens. Matter **3**, 3677 (1991)
20. A.B. Kulakov, A.A. Zhokhov, G.A. Emel'chenko, N.V. Klassen, J. Cryst. Growth **151**, 107 (1995)
21. D.S. Rimai, R.J. Sladek, Solid State Commun. **31**, 473 (1979)
22. B.F. Naylor, J. Am. Chem. Soc. **67**, 150 (1945)
23. C.E. Derrington, A. Navrotsky, M. O'Keeffe, Solid State Commun. **18**, 47 (1976)
24. M. Griffel, J.W. Stout, J. Am. Chem. Soc. **72**, 4351 (1950)
25. T.H. Yeom, Y.H. Lee, T.S. Hahn, M.H. Oh, S.H. Choh, J. Appl. Phys. **79**, 1004 (1996)
26. Y.H. Lee, D.H. Kim, B.K. Ju, M.H. Song, T.S. Hahn, S.H. Choh, M.H. Oh, J. Appl. Phys. **78**, 4253 (1995)
27. K.K. Stavrev, K.D. Nynev, G.St. Nikolov, J. Cryst. Growth **101**, 376 (1990)
28. K.K. Stavrev, S.I. Ivanov, K.D. Kvnev, G. St. Nikolov, J. Solid State Chem. **86**, 136 (1990)
29. W. Hayes, D.A. Jones, Proc. Phys. Soc. **71**, 503 (1958)
30. A.J. Tench, R.L. Nelson, Proc. Phys. Soc. **92**, 1055 (1967)
31. P. Thangadurai, S. Ramasamy, R. Kesavamoorthy, J. Phys.: Condens. Matter, **17**, 863 (2005)